Original scientific paper

Informacije MIDEM
Journal of Microelectronics,
Electronic Components and Materials
Vol. 46, No. 4(2016), 176 – 182

Lithography-Free, Crystal-Based Multiresonant Lamb Waves for Reconfigurable Microparticle Manipulation

Amgad R. Rezk and Leslie Y. Yeo

Micro/Nanophysics Research Laboratory, School of Engineering, RMIT University, Melbourne, Australia

Abstract: Acoustic wave microfluidic devices, in particular those that exploit the use of surface acoustic waves (SAWs), have been demonstrated as a powerful tool for driving microfluidic actuation and bioparticle manipulation. A limitation of these devices, however, is the requirement for the fabrication of interdigital transducer electrodes on the piezoelectric substrate, which upon excitation of an AC electrical signal at resonance, generates the SAW.

Not only is the lithographic fabrication a costly and cumbersome step, the necessity for driving the interdigitated transducers (IDTs) at resonance means that the device typically operates at a single frequency at its fundamental resonant state; the higher harmonics that may be available are often weak and negligible. As such, reconfiguring a device for different operating frequencies is usually difficult and almost always avoided. Here, we show a Lamb wave device which can mimic the microfluidic actuation and particle manipulation of SAW devices, but which can be fabricated without requiring any lithographic procedures. Moreover, we show that a large number of resonances are available, whose modes depends on harmonics associated with the substrate thickness, and, in particular, demonstrate this utility briefly for reconfigurable particle patterning.

Keywords: acoustics; microfluidics; particle manipulation; concentration

Generiranje multi-resonančnih Lamb akustičnih valov za manipulacijo bioloških delcev

Izvleček: Mikrofluidne platforme ki uporabljajo za aktuacijo zvočno valovanje ter še posebej tiste, ki izkoriščajo uporabo površinskih zvočnih valov (angl surface acoustic waves - SAW.), so se izkazali kot zelo primerno orodje za manipulacijo bioloških delcev. Omejitev pri teh napravah je zahteva za izdelavo prstastih elektrod, t.j. elektroakustičnih pretvornikov na osnovni piezoelektrični podlagi, ki ob vzbujanje z izmeničnim električnim signalom v resonanci generirajo površinske akustične valovanje. Uporaba fotolitografskega postopka pri izdelavi vzbujevalne prstaste elektrodne strukture je eden bolj zahtevnih korakov. Poleg tega prstasta struktura deluje le na osnovni resonančni frekvenci, višji harmoniki, ki so lahko na voljo, pa so pogosto šibki in zanemarljivi. Preoblikovanje prstastih struktur, ki bi omogočalo delovanje na različnih delovnih frekvencah na isti mikrofluidni platformi je ponavadi težko izvedljivo in se ne uporablja. V tem prispevku bomo predstavili enostaven način generiranja Lamb valovanja, ki omogoča transport in manipulacijo bioloških delcev na piezoelektrični podlagi in ga je možno realizirati brez fotolitografskega postopka. Poleg tega bomo v prispevku pokazali, da je možna vzpostavitev različnih resonančnih frekvenc in višjih harmoničnih komponent v povezavi s spreminjanjem debeline substrata. Obenem bomo demonstrirali uporabnost takega pristopa za poljubno manipulacijo delcev.

Ključne besede: akustični valovi; mikrofluidika; manipulacija delcev; koncentracije

** Corresponding Author's e-mail: leslie.yeo@ rmit.edu.au*

1 Introduction

The ability to manipulate (e.g., concentrate, sort and separate) particulate suspensions, particularly those pertaining to biological substances such as cells, is indispensable to microfluidic operations, where applications pertaining to biomedicine and biotechnology such as point-of-care diagnostics, biosensing, drug

development, drug delivery and tissue engineering feature prominently [1-3]. Many microfluidic strategies have been proposed for manipulating such microparticles, including the use of inertia [4], electrokinetic [5], optical [6], magnetic [7] and acoustic [8] forces, among others.

While many *bulk* acoustic microfluidic methods for particle manipulation have been proposed [8], their long wavelengths associated with the kHz order frequencies typically employed, and the necessity for large ultrasonic transducers place considerable limitations to miniaturisation and integration into chip-scale devices. More recently, surface acoustic waves (SAWs), which are the high frequency (MHz order) *surface* counterpart of *bulk* ultrasonic waves, have been shown to be an extremely powerful tool for microfluidic actuation and particle manipulation [9-12]. In the latter, standing SAWs have primarily been used for trapping particles at nodal or antinodal positions in microchannels for a myriad of applications including single cell and organism focusing, patterning and separation [13,14], even in three-dimensions [15,16]. Additionally, travelling SAWs have also been recently shown to be highly useful for particle manipulation [17-19]. Besides the above, which rely on the acoustic radiation force imparted on particles to manipulate them, particle concentration and sorting have also been demonstrated by exploiting the hydrodynamic drag force imparted on the particle by SAW-driven microcentrifugation flows [20-23].

Nevertheless, high frequency (MHz order) SAWs require cumbersome processes associated with lithography, typically achieved by metal deposition, photoresist coating, UV-exposure and wet etching, in order to fabricate the interdigitated transducers (IDTs) on the piezoelectric substrate that are required to generate the SAWs. These long multi-step procedures are not only time consuming and require skilled technicians, but also involves the additional expense of operating within a cleanroom environment. Moreover, as the SAW frequency is increased closer towards GHz order [24,25], the IDT dimensions become progressively smaller given that they correlate with the SAW wavelength, necessitating even more elaborate fabrication such as electron beam or nanoimprint lithography if robust devices are desired. Furthermore, once a device is fabricated, it typically runs on a single SAW resonant frequency, thus limiting many potential microfluidic applications, especially for reconfigurable particle manipulation within liquid drops. We note the possibility of exciting multiple frequencies on a SAW device using a single tapered IDT (TIDT) design [26] (also known as slanted-finger interdigital transducers (SFITs) [27]), although the limitation with such devices is that the width of the SAW that can be produced for a given frequency is confined to a lateral dimension that is on the order of its wavelength—typically too narrow to drive any meaningful microfluidic actuation on the scale of a droplet or channel in most cases.

Here, we briefly demonstrate the possibility for on-chip reconfigurable microparticle actuation using a simple fabrication step that does not require lithographic procedures. This extends on our previous work that showed, quite counterintuitively and contrary to long-standing practice, that it is possible to generate Lamb waves for microfluidic actuation on a piezoelectric (lithium niobate; $LiNbO_3$) substrate simply with the use of aluminium foil placed in contact with the substrate [28-30].

2 Method

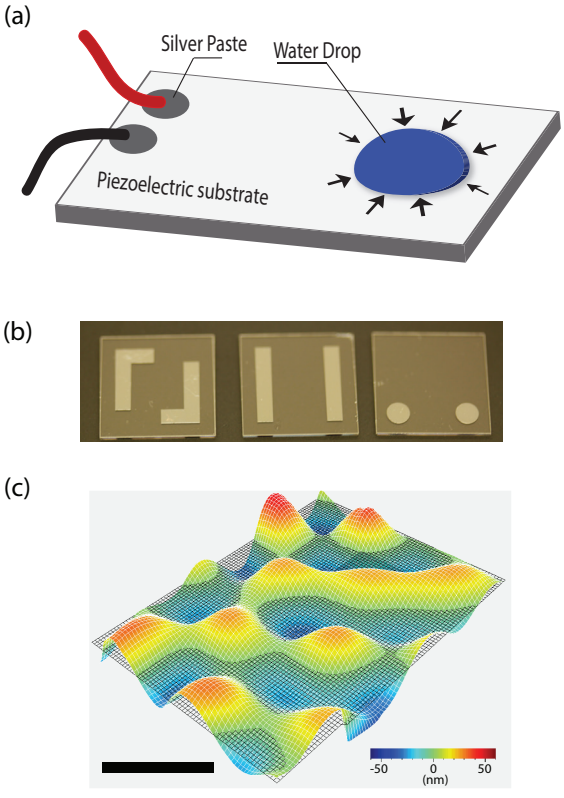

Figure 1: (a) Schematic illustration and (b) images of various electrode patterns on the lithography-free $LiNbO_3$ chip. (c) Laser Doppler Vibrometer (LDV) scan of the chip at 3.5 MHz; the scale bar denotes a length of approximately 1 mm.

The simple lithography-free setup is shown schematically in Figure 1a, wherein either conductive silver paste was spotted, or an arbitrary electrode pattern (such as the straight, L-shaped or circular patterns in

Figure 1b) comprising a conductive aluminium layer deposited with the aid of masking tape, onto the $LiNbO_3$ chip. To generate the Lamb wave in the substrate, we simply connect these electrodes to an AC source at an appropriate resonant frequency, a number of which exists, as will be discussed below. To demonstrate the possibility for reconfigurable microparticle manipulation, we placed a 5 µl sessile liquid drop comprising 3 µm polystyrene particles suspended in water at a concentration of 10^5 onto the device and observe its behaviour as a function of the applied frequency using a DSLR camera (Canon D50, Tokyo, Japan) which was connected to a long working distance microscopic lens (K2/SC, Infinity, Boulder, CO). The mechanical vibration displacement was acquired using laser Doppler vibrometry (LDV; MSA-400 and UHF-120; Polytec, Germany) whereas electrical characteristics of the device, namely the insertion loss parameter S_{11}, was measured using a vector network analyser (VNA; ZNB4, Rohde & Schwarz, Germany).

3 Results & Discussion

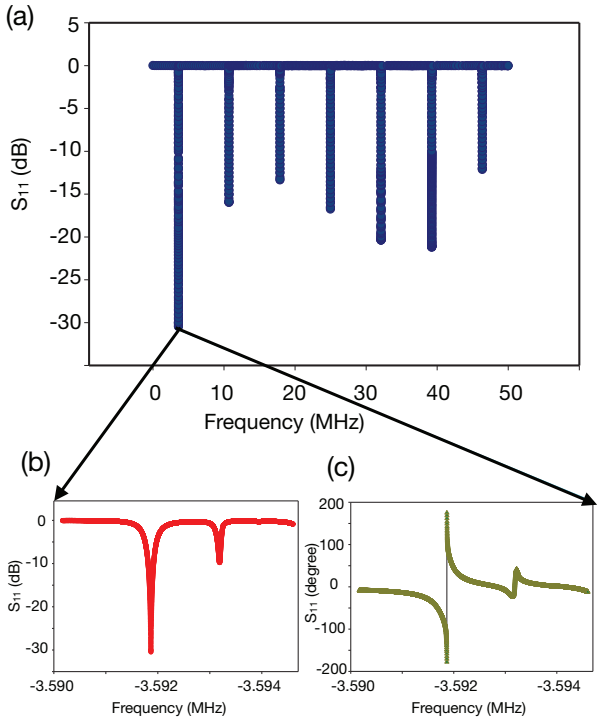

Figure 2: (a) Results from the VNA frequency sweep to measure the insertion loss parameter S_{11} of the device, which clearly shows multiple resonances starting from the fundamental resonance at 3.5 MHz, as determined from the magnification of (b) the magnitude and (c) the phase angle, and higher harmonics at every additional 7 MHz.

The VNA measurement for the insertion loss parameter S_{11} in Figure 2 shows that the device possesses multiple resonant frequencies, starting from the fundamental frequency at 3.5 MHz, and additional higher resonant modes at increments of approximately every 7 MHz. While we only show results for the frequency sweep across a range from 1 to 50 MHz in Figure 2 for clarity, discernible resonant peaks were observed even beyond 300 MHz. It is worth noting, that these resonances are insensitive to the electrode shape (dot, straight, L-shaped, circular, etc.) or their dimension, since the electric field, which is coupled to the mechanical field, traverses *vertically* through the chip thickness; the resonances are therefore only sensitive to the thickness of the substrate. Reducing this by lapping the device using a rotating wheel covered with abrasive slurry led to increases in the fundamental resonant frequency. In particular, given the speed of sound through $LiNbO_3$ c = 3500 m/s and for a substrate thickness T = 500 µm, the fundamental resonant frequency that arises can be computed from $f = \lambda c$ in which the wavelength $\lambda/2$ corresponds to T such that f = 3.5 MHz. Subsequent higher harmonics can then be obtained for $3\lambda/2$, $5\lambda/2,\ldots,(2n+1)\lambda/2$ ($n = 0, 1, 2,\ldots$) leading to resonances at every interval of 7 MHz, i.e., 10.5 MHz, 17.5 MHz,…, etc.

We also note that the proposed chip configuration in Figure 1 possesses an outstanding quality factor Q of approximately 13,000 (in contrast to that of typical SAW devices where Q factors as low as 100 are not uncommon), which not only makes it a very efficient device for microfluidic manipulation, as will describe later, but also renders it as a very sensitive platform for biosensing. Given the optical smoothness of the $LiNbO_3$ substrate and the uniformity of its thickness, which sets the wavelength, it is perhaps of little surprise that the resonant band (and hence the high quality factor) is very sharp and almost comparable to those of quartz crystals. Such crystals with high quality factor, although extremely sensitive to mass loading (which makes them very efficient sensors), however possess extremely low electromechanical coupling coefficients k_t^2, and therefore, a low figure of merit FOM = Qk_t^2. Remarkably, however, the present device, when excited at the fundamental resonant frequency, shows a reasonable value for k_t^2 of 0.8%. Although other piezoelectric substrates such as lead zirconium titanate (PZT) possess k_t^2 values up to 20%, we note that the FOM = 13,000 x 0.8% ≈ 10,000 surpasses any other piezoelectric material we know of; for example, a typical SAW on 128 YX $LiNbO_3$ with $Q \approx 100$ and $k_t^2 = 5.3\%$, has an FOM ≈ 500, considerably below that here. This suggests that the Lamb wave device is not just simple and low cost to fabricate, but also satisfies a rare requirement for any

piezoelectric substrate of being *both* a very sensitive as well as a very effective actuator.

Upon excitation of the device at the fundamental resonant frequency, i.e., 3.5 MHz, standing Lamb waves in the form of a checkerboard pattern are generated in the device with a wavelength of 1000 μm as seen in Figure 1c. We note that the presence of the liquid drop will distort this standing wave pattern due to its mass loading given that the liquid thus acts as a sink in absorbing the waves along its circular periphery [29]. Unlike previous investigations where we showed that these Lamb waves led to the generation of poloidal flows in the drop, which, in turn gave rise to the formation of toroidal particle rings [29,30], the low excitation powers (<50 mW) primarily used in this study rendered acoustic streaming in the drop insignificant, and, as such, the particles suspended in the liquid were only subjected to acoustic radiation forces instead of the dominant hydrodynamic drag.

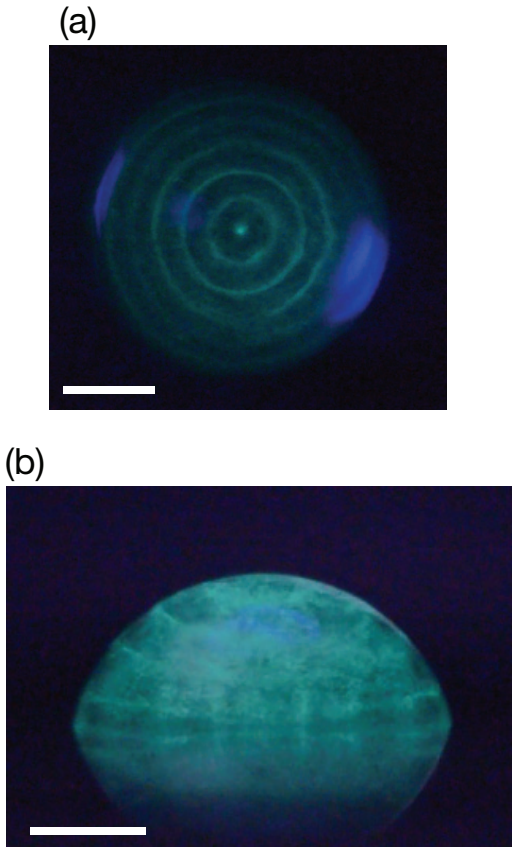

Figure 3: (a) Top and (b) side view of the three-dimensional concentric particle patterns that arise under Lamb wave substrate excitation of a 5 μl sessile liquid drop comprising 3 μm particles suspended in water at the fundamental resonant frequency, i.e., 3.5 MHz. The spacing between the concentric rings is approximately 270 μm. Scale bars denote a length of approximately 1 mm.

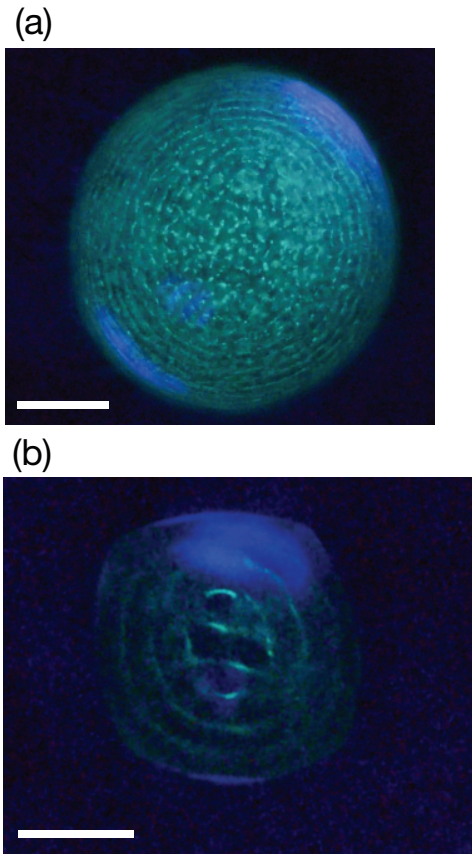

Figure 4: Top view of the three-dimensional concentric particle patterns that arise under Lamb wave substrate excitation of (a) a circular, and, (b) a roughly square 5 μl sessile liquid drop comprising 3 μm particles suspended in water at 10.5 MHz. The spacing between the concentric rings is approximately 90 μm. Scale bars denote a length of typically 1 mm.

Figure 3 shows the resultant particle patterns that arise on the free surface of the drop as well as within its bulk due to their alignment along nodal lines or planes of the standing acoustic wave that is generated as a consequence of the radiation force it imparts on the particles; the standing wave arising due to the reflections at the drop boundaries. The concentric patterns, in particular, reflect the radial nodes associated with the breathing mode of the drop, and the 270 μm spacing between the concentric particle rings correspond to a separation length of λ/2, as expected.

What distinguishes the present devices from other acoustic devices, however, is the possibility of triggering a large number of higher harmonic frequencies with reasonable efficiency, thus allowing the possibility of reconfiguring the spacing and assembly of the particle patterns *in situ*. As a brief example, Figure 4a shows the concentric particle patterns when a higher harmonic (10.5 MHz) is excited in the same device

wherein the spacing between the concentric rings has decreased to approximately 90 μm, again corresponding to λ /2 at this harmonic frequency. Higher harmonics led to smaller spacing, although the pattern cannot be resolved spatially while imaging the whole drop and is hence not shown. Such reconfigurability is in sharp contrast to SAW devices, whose excitation relies on the IDT dimensions, or bulk acoustic wave (BAW) devices in which the excitation is achieved by coating electrodes on the top and bottom surface of the piezoelectric ceramic, e.g., PZT. In those cases, the resonant excitation is predominantly limited to the fundamental resonant frequency set by the IDT (in the case of the SAW) or the substrate thickness (in the case of the bulk piston vibration). Although, theoretically, PZT can support higher harmonics effectively, the poor surface roughness of the material leads to much broader resonance (and hence low *Q* of approximately 100 and even down to about 10) for the higher harmonics, and therefore the coupling is extremely ineffective.

To illustrate that the standing waves within the drop that arise due to the reflection off its boundaries, and that it is these that assume the dominant role in determining the particle pattern rather than the underlying vibration pattern on the substrate, we rendered the $LiNbO_3$ substrate surface hydrophobic (with a Teflon coating) save for a roughly square region (with the aid of a mask during coating) on which we placed the drop. As seen in Figure 4b, the resulting particle pattern within the roughly square shaped drop is altered and closely resembles the drop contour.

Finally, we demonstrate the possibility of efficiently generating acoustic streaming, and, in particular, microcentrifugation flows, in these devices even at these higher harmonics, which cannot be achieved either using the SAW or BAW devices given the extremely weak higher harmonics in those devices, particularly given the ineffective higher harmonic coupling evident (both *Q* and k_t^2 exponentially decay with frequency). Figure 5 shows the particle concentration as a consequence of the azimuthal acoustic (Eckart) streaming within the drop, whose underlying mechanism we have discussed elsewhere [20-23], when the substrate is excited at much higher harmonics, i.e., 150 MHz, at large applied powers (approximately 500 mW) that give rise to larger substrate vibration displacements. In addition to the large streaming velocities, typically on the order of 0.5–1 mm/s observed, it can be seen that the bipolar vortex gave rise to particle concentration in two distinct islands. The ability to trigger these higher frequencies even with such a simple device then constitutes a considerable advantage given the need to date for elaborate lithographic procedures (e.g., electron beam or nanoimprint lithography) to fabricate sufficiently robust electrodes for high frequency operation [24,25].

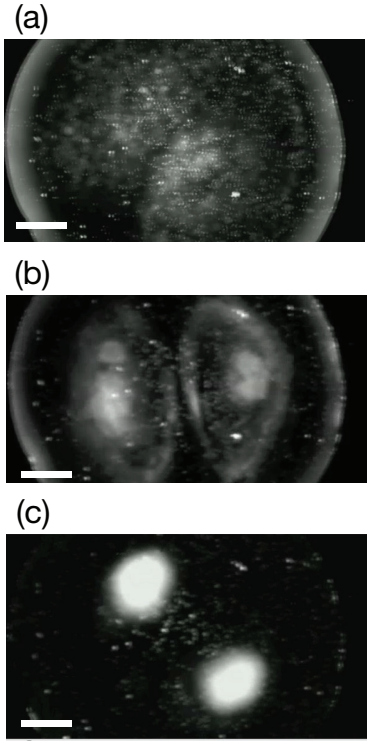

Figure 5: Bipolar vortex acoustic streaming flow is generated in a 5 μl sessile liquid drop comprising 3 μm particles suspended in water by exciting vibration in the substrate at a harmonic resonant frequency of 150 MHz with large input powers (approximately 500 mW). This leads to rapid concentration of the particles into two particle islands through particle shear induced migration [20-23]. The left image (a) shows the drop prior to excitation at time $t = 0$ wherein the particles are dispersed throughout the drop, the centre image (b) shows the bipolar vortices in the drop at $t = 1$ s during Lamb wave excitation, and the right image (c) shows the drop immediately after excitation at $t = 5$ s wherein the particles have concentrated and the substrate vibration relaxed. Scale bars denote lengths of approximately 0.5 mm.

4 Conclusion

By exploiting the large number of resonances associated with the Lamb wave vibration through the thickness of a substrate comprising a piezoelectric material, namely, lithium niobate, and its extremely high quality factor and hence figure of merit, we show the possibility of reconfigurable microfluidic actuation and particle manipulation on a single device. In doing so, we not only demonstrate the possibility of replicating the capabilities of surface acoustic wave devices with a simple electrode design that does not require lithographic

processes for fabrication but also circumvents the need for distinct devices whenever a different frequency and hence wavelength is desired.

5 References

1. G. M. Whitesides. The Origins and Future of Microfluidics. *Nature* 442, 368–373 (2006).
2. E. K. Sackmann, A. L. Fulton and D. J. Beebe. The Present and Future Role of Microfluidics in Biomedical Research. *Nature* 507, 181–189 (2014).
3. L. Y. Yeo, H.-C. Chang, P. P. Y. Chan and J. R. Friend. Microfluidic Devices for Bioapplications. *Small* 7, 12–48 (2011).
4. D. Di Carlo, D. Irimia, R. G. Tompkins and M. Toner. Continuous Inertial Focusing, Ordering, and Separation of Particles in Microchannels. *Proc. Natl. Acad. Sci. USA* 104, 18892–18897 (2007).
5. H.-C. Chang and L. Y. Yeo. *Electrokinetically-Driven Microfluidics and Nanofluidics* (Cambridge University, Cambridge, 2010).
6. K. Dholakia, P. Reece and M. Gu. Optical Micromanipulation. *Chem. Soc. Rev.* 37, 42–55 (2008).
7. N. Pamme, J. C. T. Eijkel and A. Manz. On-Chip Free-Flow Magnetophoresis: Separation and Detection of Mixtures of Magnetic Particles in Continuous Flow. *J. Magn. Magn. Mater.* 307, 237–244 (2006).
8. T. Laurell, F. Petersson and A. Nilsson. Chip Integrated Strategies for Acoustic Separation and Manipulation of Cells and Particles. *Chem. Soc. Rev.* 36, 492–506 (2007).
9. L. Y. Yeo and J. R. Friend. Surface Acoustic Wave Microfluidics. *Annu. Rev. Fluid Mech.* 46, 379–406 (2014).
10. S.-C. S. Lin, X. Mao and T. J. Huang. Surface Acoustic Wave (SAW) Acoustophoresis: Now and Beyond. *Lab Chip* 12, 2766–2770 (2012).
11. G. Destgeer and H. J. Sung. Recent Advances in Microfluidic Actuation and Micro-Object Manipulation via Surface Acoustic Waves. *Lab Chip* 15, 2722–2738 (2015).
12. J. Nam, H. Lim and S. Shin. Manipulation of Microparticles Using Surface Acoustic Wave in Microfluidic Systems: A Brief Review. *Korea-Aust. Rheol. J.*23, 255–267 (2011).
13. X. Ding, S.-C. S. Lin, B. Kiraly, H. Yue, S. Li, I-K. Chiang, J. Shi, S. J. Benkovic and T. J. Huang. On-Chip Manipulation of Single Microparticles, Cells, and Organisms Using Surface Acoustic Waves. *Proc. Natl. Acad. Sci. USA* 109, 11105–11109 (2012).
14. D. J. Collins, B. Morahan, J. Garcia-Bustos, C. Doerig, M. Plebanski and A. Neild. Two-Dimensional Single-Cell Patterning with One Cell Per Well Driven by Surface Acoustic Waves. *Nat. Commun.* 6, 8686 (2015).
15. J. Shi, S. Yazdi, S.-C. S. Lin, X. Ding, I-K. Chiang, K. Sharp and T. J. Huang. Three-Dimensional Continuous Particle Focusing in a Microfluidic Channel via Standing Surface Acoustic Waves (SSAW). *Lab Chip* 11, 2319–2324 (2011).
16. F. Guo, Z. Mao, Y. Chen, Z. Xie, J. P. Lata, P. Li, L. Ren, J. Liu, J. Yang, M. Dao, S. Suresh and T. J. Huang. *Proc. Natl. Acad. Sci. USA* 113, 1522–1527 (2016).
17. G. Destgeer, S. Im, B. H. Ha, J. H. Jung, M. A. Ansari and H. J. Sung. Adjustable, Rapidly Switching Microfluidic Gradient Generation Using Focused Travelling Surface Acoustic Waves. *Appl. Phys. Lett.* 104, 023506 (2014).
18. J. Behren, S. Langelier, A. R. Rezk, G. Lindner, L. Y. Yeo and J. R. Friend. Microscale Anechoic Architecture: Acoustic Diffusers for Ultra Low Power Microparticle Separation Via Traveling Surface Acoustic Waves. *Lab Chip* 15, 43–46 (2015).
19. D. J. Collins, A. Nield and Y. Ai. Highly Focused High-Frequency Travelling Surface Acoustic Waves (SAW) for Rapid Single-Particle Sorting. *Lab Chip* 16, 471–479 (2016).
20. H. Li, J. R. Friend and L. Y. Yeo. Surface Acoustic Wave Concentration of Particle and Bioparticle Suspensions. *Biomed. Microdev.* 9, 647–656 (2007).
21. R. Shilton, M. K. Tan, L. Y. Yeo and J. R. Friend. Particle Concentration and Mixing in Microdrops Driven by Focused Surface Acoustic Waves. *J. Appl. Phys.* 104, 014910 (2008).
22. R. V. Raghavan, J. R. Friend and L. Y. Yeo. Particle Concentration via Acoustically Driven Microcentrifugation: MicroPIV Flow Visualization and Numerical Modelling Studies. *Microfluid. Nanofluid.* 8, 73–84 (2010).
23. P. R. Rogers, J. R. Friend and L. Y. Yeo. Exploitation of Surface Acoustic Waves to Drive Size-Dependent Microparticle Concentration Within a Droplet. *Lab Chip* 10, 2979–2985 (2010).
24. M. B. Dentry, L. Y. Yeo and J. R. Friend. Frequency Effects on the Scale and Behavior of Acoustic Streaming. *Phys. Rev. E* 89, 013203 (2014).
25. R. J. Shilton, M. Travagliati, F. Beltram, M. Cecchini. Nanoliter-Droplet Acoustic Streaming via Ultra High Frequency Surface Acoustic Waves. *Adv. Mater.* 26, 4941–4946 (2014).
26. T. Frommelt, M. Kostur, M. Wenzel-Schäfer, P. Talkner, P. Hänggi and A. Wixforth. Microfluidic Mixing via Acoustically Driven Chaotic Advection. *Phys. Rev. Lett.* 100, 034502 (2008).
27. X. Ding, J. Shi, S.-C. S. Lin, S. Yazdi, B. Kiraly and T. J. Huang. Tunable Patterning of Microparticles and Cells Using Standing Surface Acoustic Waves. *Lab Chip* 12, 2491–2497 (2012).

28. A. R. Rezk, J. R. Friend and L. Y. Yeo. Simple, Low Cost MHz-Order Acoustomicrofluidics Using Aluminium Foil Electrodes. *Lab Chip* 14, 1802–1805 (2014).
29. A. R. Rezk, L. Y. Yeo and J. R. Friend. Poloidal Flow and Toroidal Particle Ring Formation in a Sessile Drop Driven by Megahertz Order Vibration. *Langmuir* 30, 11143–11247 (2014).
30. G. Destgeer, B. Ha, J. Park and H. J. Sung. Lamb Wave-Based Acoustic Radiation Force-Driven Particle Ring Formation Inside a Sessile Droplet. *Anal. Chem.* 88, 3976–3981 (2016).

Arrived: 31. 08. 2016
Accepted: 22. 09. 2016